

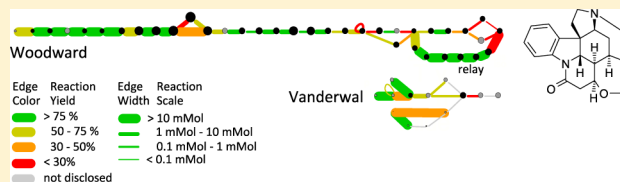
# Reaction Schemes Visualized in Network Form: The Syntheses of Strychnine as an Example

John R. Proudfoot\*

Boehringer Ingelheim Pharmaceuticals, Inc., 900 Ridgebury Road, P.O. Box 368, Ridgefield, Connecticut 06877, United States

## Supporting Information

**ABSTRACT:** Representation of synthesis sequences in a network form provides an effective method for the comparison of multiple reaction schemes and an opportunity to emphasize features such as reaction scale that are often relegated to experimental sections. An example of data formatting that allows construction of network maps in Cytoscape is presented, along with maps that illustrate the comparison of multiple reaction sequences, comparison of scaffold changes within sequences, and consolidation to highlight common key intermediates used across sequences. The 17 different synthetic routes reported for strychnine are used as an example basis set. The reaction maps presented required a significant data extraction and curation, and a standardized tabular format for reporting reaction information, if applied in a consistent way, could allow the automated combination of reaction information across different sources.



Reaction schemes presented in a network form facilitate comparison. Examples are given from the syntheses of strychnine.

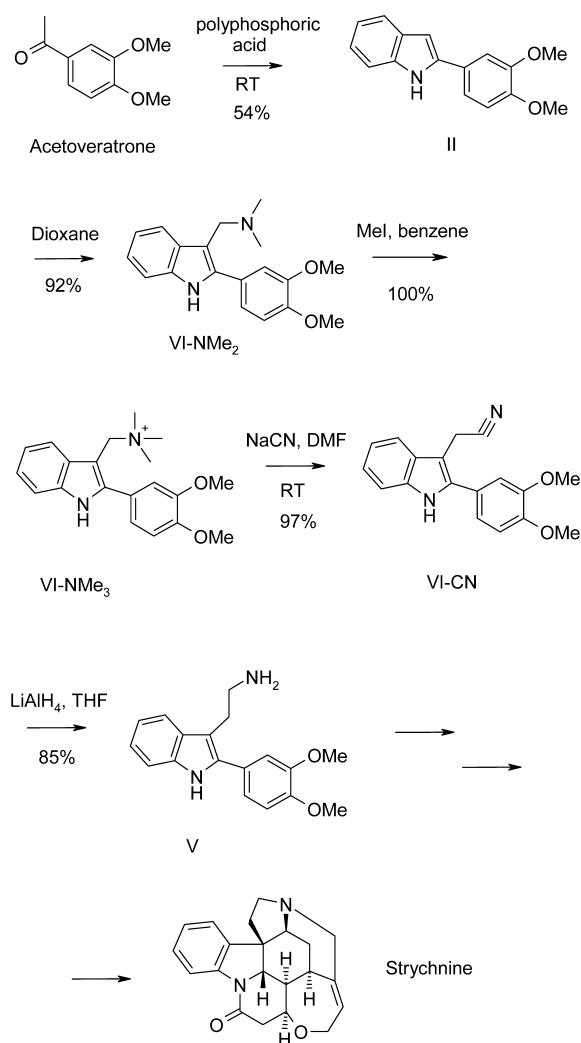
Reaction schemes that show multi-step organic syntheses generally take the form shown in Scheme 1, in which the structures of reactants and products are connected by arrows with reaction conditions and product yields as annotations. For any individual reaction sequence, these representations convey the structural changes involved with varying degrees of clarity; however, they are less successful for comparisons of multiple sequences. Certain reactant features such as molecular size, which might be useful as an indicator of atom economy throughout a sequence, are often obscured by the abbreviated representations used for protecting groups; other features such as throughput or scale or degree of characterization and physical form of the reactants are rarely presented explicitly and are usually left to an experimental section or Supporting Information. Alternative representations of reaction schemes, specifically those that are network-like, have appeared occasionally, and recent examples demonstrate a potential to transform the visualization and exploration of molecular transformations.<sup>1</sup> A number of earlier network-like representations of individual or multiple reaction sequences highlighted molecular features such as complexity<sup>2,3</sup> or sequence features such as convergence.<sup>4,5</sup> One limiting aspect of the earlier representations was the requirement to graph by hand the representation for the particular schemes of interest. While feasible for a limited application, this would be time consuming for any broader exercise. We were interested in expanding the network representation of reaction sequences, analogous to those disclosed recently,<sup>1</sup> to a form suitable for comparing multiple schemes. In particular, we aimed to take advantage of the features of the available open source network visualization tool, Cytoscape,<sup>6</sup> to represent reaction and reactant attributes.

Cytoscape has been used to represent chemical structure and property information such as the relationships between

compounds in computed clusters<sup>7</sup> and the mapping of drug-target relationships.<sup>8</sup> As shown below with a test set of the reported syntheses of strychnine, it can also be used to map and compare reaction sequences. Numerous reviews on the syntheses of strychnine are available, and these typically highlight key or unique disconnections or concepts in the reaction sequences.<sup>9</sup> However, it is often challenging to comprehend the relationships between the different approaches, and one particular goal of this exercise was to develop representations that would allow straightforward comparisons while providing the capacity to highlight features that are rarely covered in review articles.

The sequence shown in Scheme 1, the first five steps in the Woodward synthesis of strychnine,<sup>10</sup> can be reformatted for representation as a network graph. Because network nodes and edges can be assigned to reactant and/or reaction attributes, options are available for the representation of synthesis sequences as a network. A recent directed bipartite representation,<sup>1d</sup> in which both reactants and reactions are represented as nodes, illustrated the potential to explicitly show all synthetic relationships within or across pathways including those reactions that involve multiple reactants or products. For the representations that follow, reactant attributes, and more specifically those of reactants that constitute synthesis intermediates rather than all the reactants employed in a specific transformation, are assigned to nodes. Edges are employed to render reaction attributes. The bipartite representation is comprehensive in capturing all the reagent and reaction information, while the focus of the present

Received: November 20, 2012

**Scheme 1. Structure of Strychnine and First Five Steps in Synthesis Reported by Woodward**

approach is the transformations of the key synthesis intermediates.

Table 1 presents the information in Scheme 1, expanded to all the steps in the Woodward synthesis and including some additional attributes (e.g., scale, #atoms, mp, chiral or not), in a format that allows the network representation shown in Figure 1. In Figure 1, the thickness of the lines connecting the nodes reflects the scale on which the reaction was conducted, and the color of the connecting line is set to reflect the yield. The node size is related to the number of atoms in the reactant (as a surrogate for molecular size), and the nodes are shaded according to whether or not a melting point was reported. Woodward took advantage of relay intermediates generated by degradation of strychnine, and this sequence is also represented in the map. The self-loop at node XXXIX reflects the resolution of the synthetic intermediate to provide a sample identical to the relay compound. One additional feature unique to the Woodward sequence is that, in the final step, two intermediates generated in the penultimate step are separated and recombined in the final reaction leading to strychnine. This leads to the bifurcation and recombination shown for node LXIX and that immediately below.

The application of this approach to a single short reaction sequence is clearly of limited value. However, for more

complicated situations encompassing multiple reaction schemes, it can prove informative. Figures 2–4 illustrate in analogous formats the syntheses of strychnine reported to early 2012.<sup>11–13</sup> Figure 2 presents a comparison of all the reported syntheses. Figure 3 presents a map in which scaffold changes are emphasized. Figures 4 and 5 present maps where structures common to more than one sequence are consolidated to unique nodes. As above, the following attributes were abstracted from the published syntheses in order to generate the representations: (a) reactant structure, product structure, reaction scale (mmole), reaction yield, product status (achiral, racemic or enantiomerically pure), and product melting point.<sup>14</sup> The number of atoms (num\_atoms) and the number of bridge bonds (num\_bridgebonds) which in this instance is a useful surrogate for molecular complexity were computed for each reactant.<sup>15</sup>

In completing this process, a number challenges arose in regard to generating a consistent representation of the available information. It is common practice to complete two or more reaction steps before characterization of a product and determination of yield. For these cases, the reaction scale and yield are associated with the overall transformation, but all steps in the sequence are captured along with scale and yield, if disclosed. On occasion, product yield is reported on the basis of recovered starting material. In these cases, the yield was recalculated based on the actual amount of reactant used, and the yield of recovered starting material was captured separately. Figure 2 represents all reported steps and transformations; for Figure 3, resolution and recovery steps are removed.

In Figure 2, the individual syntheses are ordered vertically by date of publication of the detailed experimental information and are aligned at the right-hand side by the node representing strychnine. Formal syntheses, i.e., those where a previously described precursor rather than strychnine itself is synthesized, are displaced leftwards by the number of steps required to complete the sequence.<sup>16</sup> Node size is related to number-of-atoms in the reactant and the line color to the reported yield (green >80% and red <30%, with additional colors as described in the legend). The nodes are shaded according to whether or not a melting point was reported for the reaction product. In this representation, the shorter vs the longer syntheses are immediately apparent, as are those that are linear rather than convergent. The disappearance over time of melting point as a criterion for compound characterization and purity, even of the final target, is also evident. Aside from the Woodward sequence, any self-loop represents a reported recovery of starting material from a reaction (e.g., Shibasaki sequence, node labeled 19). One particular feature of note is the relative brevity and convergence of the Rawal synthesis relative to the others reported between 1993 and 1995 (Magnus, Kuehne, and Overman). Four subsequent syntheses, those of Reissig, Mori, Vollhardt, and Bodwell, take advantage of a late stage precursor to isostrychnine in the Rawal synthesis; a fact that is not apparent in this particular representation but is highlighted in Figure 4.

One structural feature of strychnine that stands in contrast to many other natural product targets is the complexity of the core scaffold combined with minimal scaffold substitution. This feature of the target indicated that a representation of the synthesis strategies that focused on the scaffold changes throughout the various sequences might be informative. For the representation in Figure 3, each reactant was processed computationally to remove protecting groups and generate a modified Murcko scaffold<sup>17</sup> that retains atom types but in which all bonds are set to a single bond type. This focus on the core

Table 1. Tabulation of Data from Woodward Synthesis of Strychnine<sup>a</sup>

reactant	product	scale (mmol)	yield (%)	chiral	MP (°C)	type	num_atoms
acetoveratrone	II	138.8	54.4				13
II	VI-NME2	22.1	92		185–9		19
VI-NME2	VI-NME3	20.3	100		122–4		23
VI-NME3	VI-CN	20.3	97				24
VI-CN	V	342	85		231–4		22
V	VII	327	92		146–8		22
VII	XI	118	64.4		170–80		28
XI	XIV	11.2	85	no	145–146		38
XIV	XV	21.6	98.5	no	180–1		38
XV	XX	32	30	no	206		41
XV	XVI	2	29	no	206		41
XVI	XX	1.31	75	no	165 and 184		43
XX	XXVIII	1.4	72	no	187–8		38
XXVIII	N-acetylpyridone diacid	1.01	94.4	no	ND		25
N-acetylpyridone diacid	XXIX	0.79	84	no	275		28
XXIX	XXX	2.2	87.5	no	181–2		30
XXX	XXXII	2.03	95	no	200–205		28
XXXII	XXXV	0.43	77	no	217		38
XXXV	XXXVI	1.03	84	no	256–7		35
XXXVI	XXXVII	0.7	72.5	no	234		27
XXXVII	XXXIX	1.21	59	no	186		27
XXXIX	XXXIX	0.71	21	no	284		26
XXXIX	XL	0.57	27.5	yes	295–300		26
XL	XLIV	0.33	99	yes	260–3		29
XLIV	XLV	0.33	12.4	yes			23
XLV	LXVI	0.63	53	yes	172–4		24
LXVI	LXVII	1.45	86	yes	302–5		26
LXVII	LXVIII	0.75	30	yes	244–5		26
LXVIII	LXIX	0.51	12.5	yes	192–200		26
LXVIII	isostrychnine acetates	0.51	33	yes	192–200		26
LXIX	LXX	0.02	14	yes	208–12		25
isostrychnine acetates	LXX	0.17	14	yes			28
LXX	strychninonic acid	299	24	yes	278–85	relay	25
strychninonic acid	LVIII R = H	111	89	yes	257–9	relay	29
LVIII R = H	LVIII R = Ac	62.1	88	yes	228–31	relay	27
LVIII R = Ac	strychninolone b acetate LV	54.2	85	yes	242–4	relay	27
strychninolone b acetate LV	dehydrostrychninolone acetate	25.5	86	yes	135	relay	27
dehydrostrychninolone acetate	Dehydro strychninolone	19.3	92	yes	282–5	relay	24
Dehydro strychninolone	XLV	18.8	68	yes	228–30	relay	24
XLV	XXXVIII-acid	0.79	47.5	yes	175–80	relay	23
XXXVIII-acid	XXXIX	0.65	52	yes	305–8	relay	26

<sup>a</sup>Original numbering in the Woodward manuscript is retained whenever possible. Strychnine is represented by LXX.

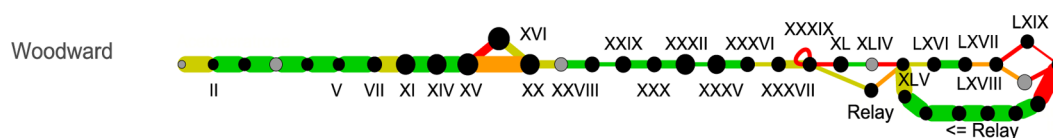
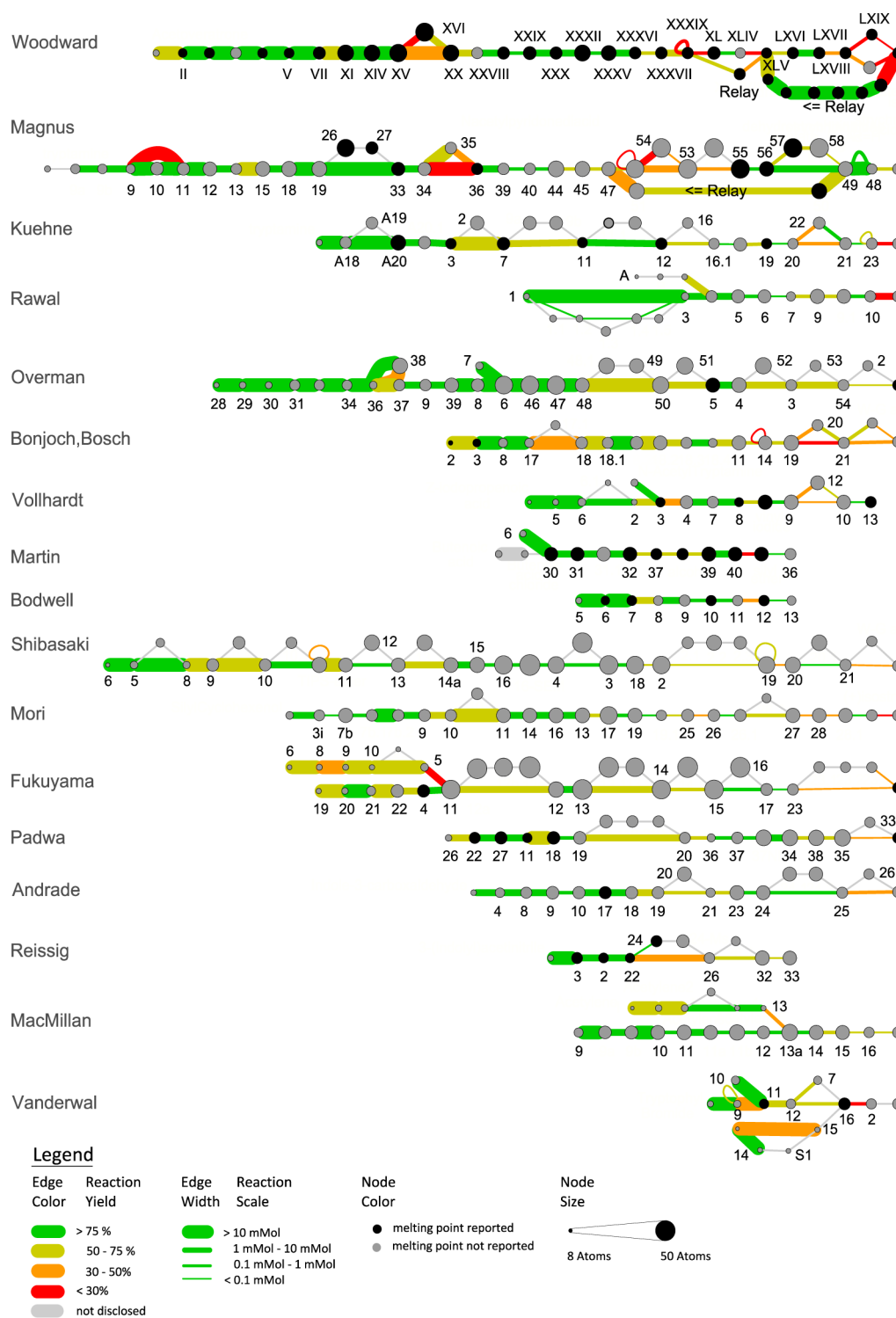


**Figure 1.** Network representation of the Woodward synthesis of strychnine. For explanation of the color scheme, see Figure 2.

scaffold of reactants provides an informative perspective on the progression toward the target scaffold of strychnine. In Figure 3, multiple transformations on the same scaffold appear as self-loops, and a new node appears only when a new scaffold is generated. From this map, one key feature that distinguishes the shorter from the longer sequences is the number of steps employed to adapt each scaffold to the appropriate functionalization state before proceeding to the next. Because of the minimal substitution on strychnine, these transformations relate exclusively to the removal of substituents (i.e., protecting

groups) or oxidation state changes on the individual scaffold intermediates. In Figure 3, nodes are shaded according to the number of bridge bonds in the scaffold. Scaffolds represented by “colorless” nodes contain no bridge bonds, and strychnine at the RHS contains the largest number of bridge bonds and is shaded black. The scaffold points at which significant complexity is introduced are readily apparent.

In the network map in Figure 1, the unique node identifier is a compound number (that from the original publication if the structure is numbered) combined with the author name, and in



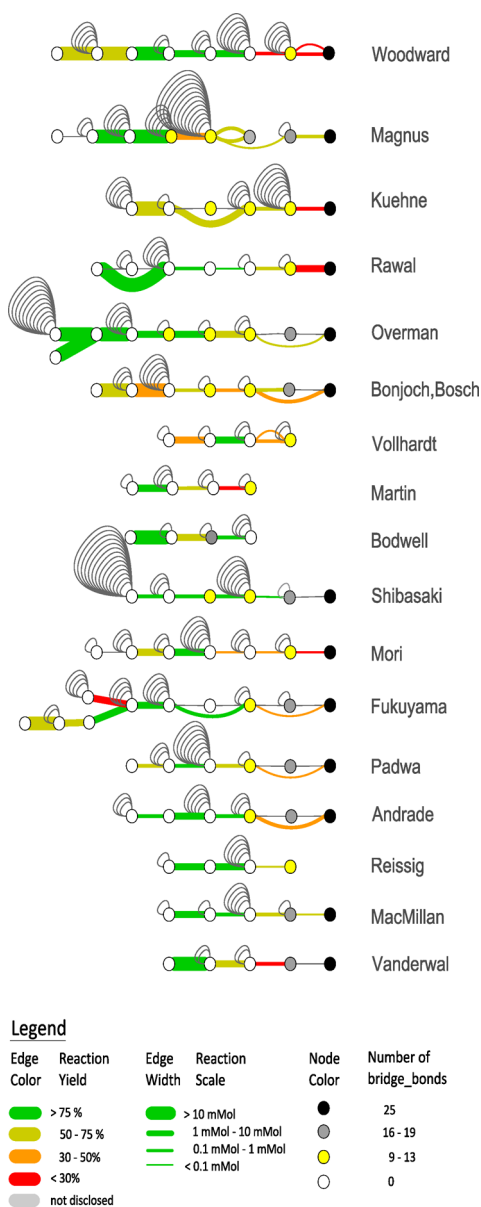
**Figure 2.** Comparative network representation of the reported syntheses of strychnine. Node size is scaled relative to the number-of-atoms in the reactant, and edges are colored in relation to the reported yield as in the legend. Edge thickness is related to the reaction scale. Nodes are shaded according to whether a melting point was reported (black) or not (gray) for the reaction product.

Figure 2, a combination of the author name and SMILES representation of the Murcko scaffold was used. These unique identifiers are adequate for the concurrent representation of separate individual schemes. However, for a network map that consolidates common intermediates to unique nodes, an identifier reflective of the chemical structure and independent of any particular numbering scheme is required. For Figure 4, a canonical SMILES string,<sup>18,19</sup> which explicitly represents the

chemical structure represented by the node, is the unique identifier. In the creation of the network map, this selection permits an automatic consolidation of structures common to multiple sequences.

The representation in Figure 4 is a manually rearranged version of an initial automatically generated layout. The number of overlapping edges has been minimized (with no change to connectivity), while maintaining the linear/convergent meta-





**Figure 3.** Reduced map of the reported syntheses of strychnine. Each node represents a separate scaffold. Each loop represents a transformation on the scaffold represented by the node.

phors usually used in depicting reaction schemes. The final appearance of this map was influenced also by an emerging similarity to idealized transportation maps. Figure 5 represents the core of Figure 4, with structures associated to key nodes. In these maps, node size is related to the number of atoms. Node colors are also related to the number of atoms, and synthetic intermediates that contain significantly more atoms than present in the target are readily apparent. The black edges are those where multiple sequences proceed from the indicated nodes.

Figures 4 and 5 emphasize the earlier point that multiple sequences proceed through key earlier common intermediates. For example, intermediate 9 from Rawal (Figure 5) was targeted by Vollhardt, Mori, Bodwell, and Reissig, and intermediate 54 from Overman was targeted by Fukuyama, Martin, Andrade, and Bonjoch. From Figures 4 and 5, it is evident that the syntheses proceed through one or other of two penultimate intermediates (isostrychnine or Wieland–Gumlich aldehyde), although they

do not capture the diversity of possible topologies available that are one ring disconnection removed from the structure of strychnine.

In Figure 6, the additional ring topologies that are one ring bond cleavage removed from strychnine are shown. The topologies shown are a subset of all those available because the aromatic character of the left-hand side ring is retained. The topologies say nothing about the difficulty or otherwise of using these systems in precursors toward strychnine. It is intriguing however that only two of the twelve topologies that are one nonaromatic ring bond cleavage removed from the target have actually been employed to date. This, at least in part, is a testament to the influence that the early degradation studies on strychnine have had on the design and implementation of synthesis strategies. Just as remarkable is the fact that most of the precursors to these two penultimate topologies (those of isostrychnine and Wieland–Gumlich aldehyde) employ just two additional topologies.

## CONCLUSION

A process for generating network-type maps for individual or multiple reaction sequences using freely available visualization tools is demonstrated. Seventeen different synthetic routes involving hundreds of intermediates are presented in concise visualizations that can highlight features not often emphasized in review articles. It is somewhat remarkable that given the topological space available for one ring bond disconnection removed from strychnine, all seventeen reported syntheses converge on one or the other of two late stage precursors: isostrychnine and Wieland–Gumlich aldehyde. This is a remarkable testament to the power that the initial degradation studies have had on influencing subsequent synthesis tactics for this target. Expression of the synthesis schemes in a form that highlights the scaffolds used emphasizes the importance of scaffold transitions in the development of short and efficient syntheses. In most of the longer syntheses, several steps are used to modify the protection or oxidation state of the initially generated scaffold before transition to the next. In the shorter syntheses, such scaffold manipulations are kept to a minimum.

The maps presented here depict multiple synthesis efforts directed toward a common target molecule. There are additional synthesis efforts where analogous representations might also be informative. Process optimization, in which different routes involving multiple experiments lead to the optimized synthesis of a discrete target molecule, could constitute one such case. Here, because there would be an increased emphasis on identifying the best reaction conditions, a bipartite map might be preferred. Another use, an example of which is in preparation, would be to represent all the reaction sequences conducted in the course of a particular project (a drug discovery project in this case) as a means to highlight not just the key discoveries that progress to success but also represent those activities that synergize with others or lead to dead ends.

Although one goal of this exercise was to develop a process for network representations of reaction sequences that is less time consuming than those reported earlier, we cannot categorically state that this has been achieved. The layouts shown above required substantial modification of the defaults available in Cytoscape in order to achieve representations reflective of the style of standard reaction sequences. The extraction and curation of the primary data used to generate the maps was also challenging, in part because experimental details are often relegated to the Supporting Information and reported in

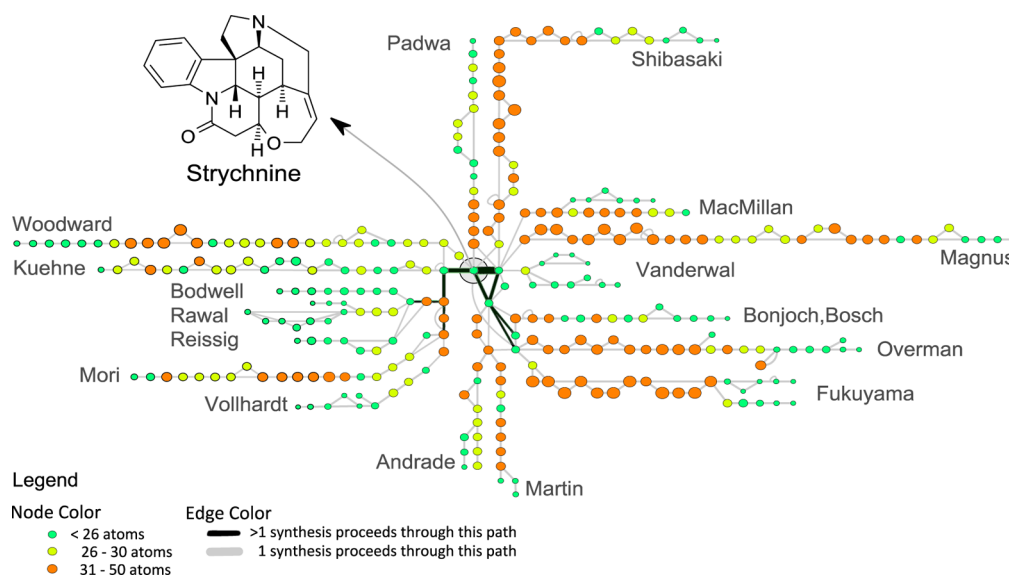


**Figure 4.** Consolidated map of the reported syntheses of strychnine. Node color and size is related to the number of atoms. The black edges are those where more than one synthesis sequence proceeds between the nodes.

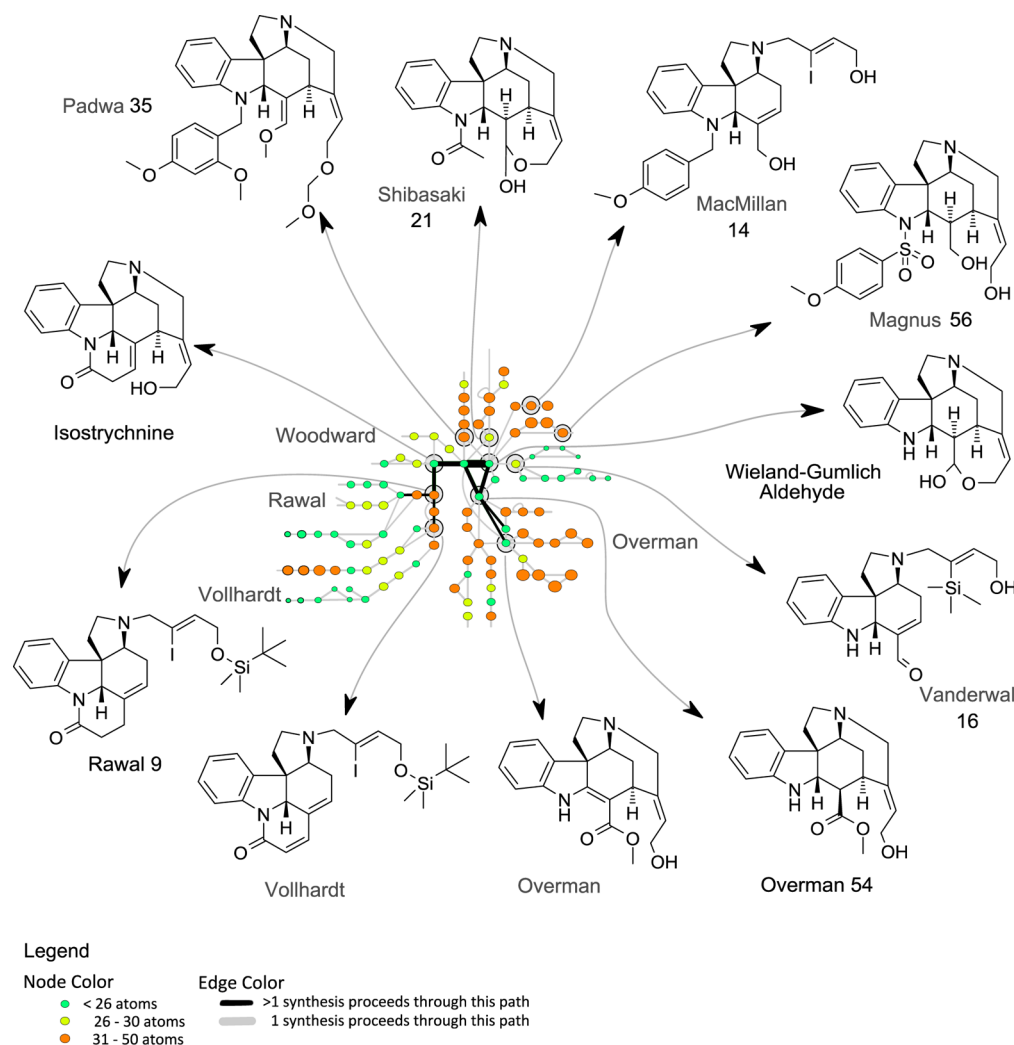


**Figure 5.** Key common intermediates in the syntheses of strychnine. Those along “black” edges are used in more than one synthesis sequence.

descriptive rather than systematic formats but also because the compound structures had to be redrawn and processed to

generate SMILES representations and computed molecular properties. Because reaction maps such as those represented here

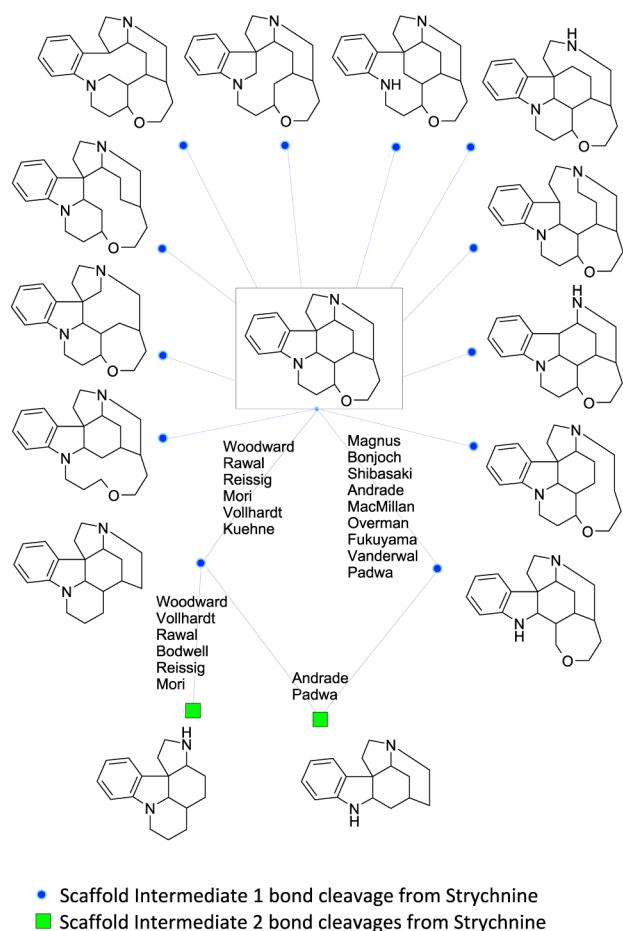


**Figure 6.** Ring topologies one and two bond cleavages removed from the strychnine scaffold.

require a highly curated basis set, perhaps a standard format for reporting reaction information should be adopted. For example, a format analogous to Table 1 with the addition of fields for reactant and product structure (INCHI or SMILES representation) applied in a consistent way could allow the automated combination of reaction information across different sources without the need for manual data extraction and extensive curation.

## ■ ASSOCIATED CONTENT

### Supporting Information

Table of the data used to generate the maps represented in Figures 1–5. This material is available free of charge via the Internet at <http://pubs.acs.org>.

## ■ AUTHOR INFORMATION

### Corresponding Author

\*Phone: +1 2037985107. Fax: +1 2037916072. E-mail: [john.proudfoot@boehringer-ingenheim.com](mailto:john.proudfoot@boehringer-ingenheim.com).

### Notes

The authors declare no competing financial interest.

## ■ ACKNOWLEDGMENTS

I thank the reviewers for the many helpful suggestions that are incorporated into the final version of this manuscript.

## ■ REFERENCES

- (1) (a) Fialkowski, M.; Bishop, K. J. M.; Chubukov, V. A.; Campbell, C. J.; Grzybowski, B. A. Architecture and evolution of organic chemistry. *Angew. Chem., Int. Ed.* **2005**, *44*, 7263–7269. (b) Grzybowski, B. A.; Bishop, K. J. M.; Kowalczyk, B.; Wilmer, C. E. The “wired” universe of organic chemistry. *Nat. Chem.* **2009**, *1*, 31–36. (c) Kowalik, M.; Gothard, C.; Drews, A. M.; Gothard, N.; Wieckiewicz, A.; Fuller, P. E.; Grzybowski, B. A.; Bishop, K. J. M. Rewiring chemistry: Algorithmic discovery and experimental validation of one-pot reactions in the network of organic chemistry. *Angew. Chem., Int. Ed.* **2012**, *51*, 7922–7927. (d) Fuller, P. E.; Gothard, C. M.; Gothard, N. A.; Wieckiewicz, A.; Grzybowski, B. A. Chemical network algorithms for the risk assessment and management of chemical threats. *Angew. Chem., Int. Ed.* **2012**, *51*, 7933–7937.
- (2) Bertz, S. H. Convergence, molecular complexity, and synthetic analysis. *J. Am. Chem. Soc.* **1982**, *104*, 5801–5803.
- (3) Whitlock, H. W. On the structure of total synthesis of complex natural products. *J. Org. Chem.* **1998**, *63*, 7982–7989.
- (4) Hendrickson, J. B. Systematic synthesis design. 6. Yield analysis and convergence. *J. Am. Chem. Soc.* **1977**, *99*, 5439–5450.
- (5) Klein, D. J.; Ivanciuc, T.; Ryzhov, A.; Ivanciuc, O. Combinatorics of reaction–network posets. *Comb. Chem. High Throughput Screening* **2008**, *11*, 723–733.
- (6) (a) Smoot, M.; Ono, K.; Ruscieski, J.; Wang, P.-L.; Ideker, T. Cytoscape 2.8: New features for data integration and network visualization. *Bioinformatics* **2011**, *27*, 431–432. (b) Cytoscape. <http://www.cytoscape.org/> (accessed March 18, 2013).
- (7) Lepp, Z.; Huang, C.; Okada, T. Finding key members in compound libraries by analyzing networks of molecules assembled by structural similarity. *J. Chem. Inf. Model.* **2009**, *49*, 2429–2443.
- (8) Chen, B.; Ding, Y.; Wild, D. J. Assessing drug target association using semantic linked data. *PLoS Comput. Biol.* **2012**, *8*, e1002574.
- (9) (a) Cannon, J. S.; Overman, L. E. Is There no end to the total syntheses of strychnine? Lessons learned in strategy and tactics in total synthesis. *Angew. Chem., Int. Ed. Engl.* **2012**, *51*, 4288–4311. (b) Bonjoch, J.; Sole, D. Synthesis of strychnine. *Chem. Rev.* **2000**, *100*, 3455–3482. (c) Beifuss, U. New total syntheses of strychnine. *Angew. Chem., Int. Ed. Engl.* **1994**, *33*, 1144–1149.
- (10) (a) Woodward, R. B.; Cava, M. P.; Ollis, W. D.; Hunger, A.; Daeniker, H. U.; Schenker, K. The total synthesis of strychnine. *J. Am. Chem. Soc.* **1954**, *76*, 4749–4751. (b) Woodward, R. B.; Cava, M. P.; Ollis, W. D.; Hunger, A.; Daeniker, H. U.; Schenker, K. The total synthesis of strychnine. *Tetrahedron* **1963**, *19*, 247–288.
- (11) (a) Magnus, P.; Giles, M.; Bonnert, R.; Kim, C. S.; McQuire, L.; Merritt, A.; Vicker, N. Synthesis of strychnine via the Wieland–Gumlich aldehyde. *J. Am. Chem. Soc.* **1992**, *114*, 4403–4405. (b) Knight, S. D.; Overman, L. E.; Pairaudeau, G. Asymmetric total syntheses of (–)- and (+)-strychnine and the Wieland–Gumlich aldehyde. *J. Am. Chem. Soc.* **1993**, *115*, 9293–9294. (c) Knight, S. D.; Overman, L. E.; Pairaudeau, G. Asymmetric total syntheses of (–)- and (+)-strychnine and the Wieland–Gumlich aldehyde. *J. Am. Chem. Soc.* **1995**, *117*, 5776–5788. (d) Kuehne, M. E.; Xu, F. Total synthesis of strychnan and aspidospermatan alkaloids. 3. The total synthesis of (±)-strychnine. *J. Org. Chem.* **1993**, *58*, 7490–7497. (e) Rawal, V. H.; Iwasa, S. A short, stereocontrolled synthesis of strychnine. *J. Org. Chem.* **1994**, *59*, 2685–2686. (f) Solé, D.; Bonjoch, J.; García-Rubio, S.; Peidró, E.; Bosch, J. Enantioselective Total synthesis of Wieland–Gumlich aldehyde and (–)-strychnine. *Chem.—Eur. J.* **2000**, *6*, 655–665. (g) Ito, M.; Clark, C. W.; Mortimore, M.; Goh, J. B.; Martin, S. F. A biomimetic approach to the strychnos alkaloids. A novel, concise synthesis of (±)-akuammicine and a route to (±)-strychnine. *J. Am. Chem. Soc.* **2001**, *123*, 8003–8010. (h) Eichberg, M. J.; Dorta, R. L.; Lamottke, K.; Vollhardt, K. P. C. The Formal Total synthesis of (±)-strychnine via a cobalt-mediated [2+ 2 + 2] cycloaddition. *Org. Lett.* **2000**, *2*, 2479–2481. (i) Mori, M.; Nakanishi, M.; Kajishima, D.; Sato, Y. A novel and general synthetic pathway to strychnos indole alkaloids: Total syntheses of (–)-tubifoline, (–)-dehydrotubifoline, and (–)-strychnine using palladium-catalyzed asymmetric allylic substitution. *J. Am. Chem. Soc.* **2003**, *125*, 9801–9807. (j) Bodwell, G. J.; Li, J. A concise formal total synthesis of

( $\pm$ )-strychnine by using a transannular inverse-electron-demand Diels-Alder reaction of a [3](1,3)indolo[3](3,6)pyridazinophane. *Angew. Chem., Int. Ed.* **2002**, *41*, 3261–3262. (k) Ohshima, T.; Xu, Y.; Takita, R.; Shimizu, S.; Zhong, D.; Shibasaki, M. Enantioselective total synthesis of (-)-strychnine using the catalytic asymmetric Michael reaction and tandem cyclization. *J. Am. Chem. Soc.* **2002**, *124*, 14546–14547. (l) Kaburagi, Y.; Tokuyama, H.; Fukuyama, T. Total synthesis of (-)-strychnine. *J. Am. Chem. Soc.* **2004**, *126*, 10246–10247. (m) Zhang, H.; Boonsombat, J.; Padwa, A. Total synthesis of ( $\pm$ )-strychnine via a [4 + 2]-cycloaddition/rearrangement cascade. *Org. Lett.* **2007**, *9*, 279–282. (n) Sirasani, G.; Paul, T.; Dougherty, W., Jr.; Kassel, S.; Andrade, R. B. Concise total syntheses of ( $\pm$ )-strychnine and ( $\pm$ )-akuammicine. *J. Org. Chem.* **2010**, *75*, 3529–3532. (o) Beemelmans, C.; Reissig, H.-U. A short formal total synthesis of strychnine with a samarium diiodide induced cascade reaction as the key step. *Angew. Chem., Int. Ed.* **2010**, *49*, 8021–8025. (p) Martin, D. B. C.; Vanderwal, C. D. A synthesis of strychnine by a longest linear sequence of six steps. *Chem. Sci.* **2011**, *2*, 649–651. (q) Jones, S. B.; Simmons, B.; Mastracchio, A.; MacMillan, D. W. C. Collective synthesis of natural products by means of organocascade catalysis. *Nature* **2011**, *475*, 185–188.

(12) The synthesis of strychnine from Professor Stork is not included because the relevant experimental details are not available. On the basis of references in publications reporting the various syntheses of strychnine, the synthesis was presented at the Ischia Advanced School of Organic Chemistry, Ischia Porto, Italy, September 21, 1992.

(13) For the Kuehne synthesis, only the endame encompassing the isostrychnine sequence is captured.

(14) Information is available in table form in the Supporting Information.

(15) Computed using components of Pipeline Pilot version 8.0; Accelrys: San Diego, CA, 2010. <http://accelrys.com/products/pipeline-pilot/> (accessed March 18, 2013).

(16) The initial reaction map was exported in svg format, and minor edits were made for clarity using Inkscape, an opensource svg editing program, [www.inkscape.org](http://www.inkscape.org) (accessed March 18, 2013).

(17) Bemis, G. W.; Murcko, M. A. The properties of known drugs. 1. Molecular frameworks. *J. Med. Chem.* **1996**, *39*, 2887–2893.

(18) Weininger, D. SMILES, a chemical language and information system. 1. Introduction to methodology and encoding rules. *Chem. Inf. Comput. Sci.* **1989**, *28*, 31–36.

(19) (a) The molecular structure is represented in SMILES format as a node attribute to take advantage of Chemviz a structure visualization plug-in for Cytoscape. <http://apps.cytoscape.org/apps/chemviz> (accessed March 18, 2013). (b) An alternative plug-in for structure visualization has also been described. Xiong, B.; Liu, K.; Wu, J.; Burk, D. L.; Jiang, H.; Shen, J. DrugViz: A Cytoscape plugin for visualizing and analyzing small molecule drugs in biological networks. *Bioinformatics* **2008**, *24*, 2117–2118.